factor, *Wnt2bb*, and that spatiotemporal control of Wnt2bb/prt expression may regulate liver specification either directly or indirectly via BMP. These findings were the first genetic evidence supporting a role for Wnt signaling in liver development. Another recent report has shown that endothelial cells can modulate the apicobasal polarization of hepatocytes during liver organogenesis.[32] Using computer-aided 3-D visual analysis of the intrahepatic and biliary vascular networks, Sakaguchi *et al.* demonstrated that the highly branched nature of these networks influences the polarization of adjacent hepatocytes.[32]

Like studies of zebrafish mutants, studies of medaka mutants have greatly contributed to our understanding of liver formation mechanisms. Our group has carried out systematic mutagenesis screens in medaka and identified 19 recessive mutations that have been assigned to five phenotypic groups (Fig. 6).[33] Group 1 contains mutations in six genes that affect the formation of endoderm, endodermal rods and the hepatic bud (including hepatoblasts). Group 2 comprises mutations in four genes that affect liver specification and liver morphogenesis. The *hiohgi (hio)* mutants of this group resemble certain zebrafish *prt* mutants, in that the liver is small and malformed. Group 3 consists of mutations in three genes that affect the laterality of the liver. In the *kendama* mutants of this group, the laterality of the heart and liver is uncoupled and randomized. Group 4 includes mutations in three genes that alter bile color, indicative of defects in hemoglobin–bilirubin metabolism and globin synthesis. Group 5 contains mutations in three genes that result in decreased accumulation in the gall bladder of PED6, a fluorescent metabolite of a phospholipase A2 substrate. This phenotype implies that these

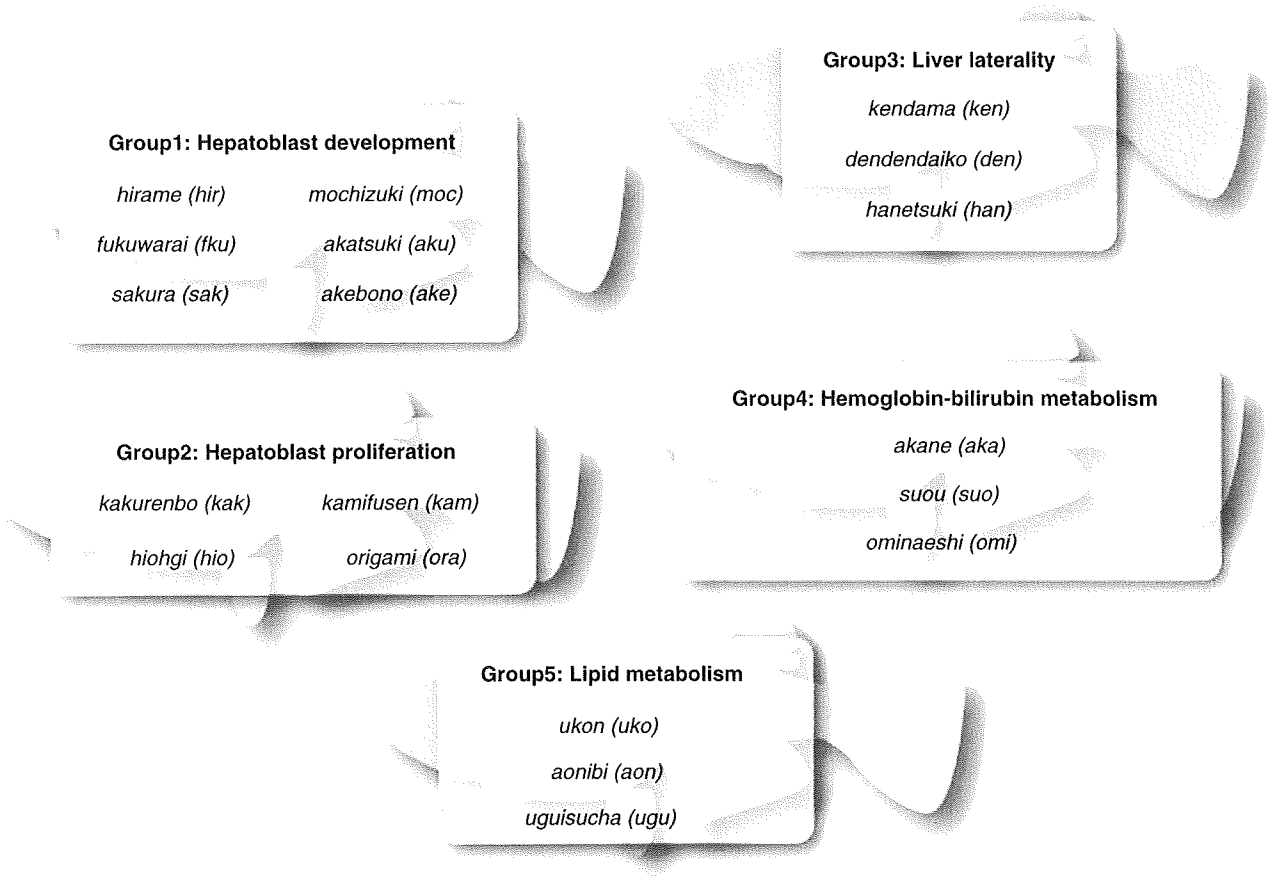

Figure 6 Liver mutations in medaka. The recessive mutations listed were classified into five phenotypic groups based on their impairment of the indicated aspects of liver development or function.

genes are involved in either lipid metabolism or the transport of lipid metabolites. Our goal is to translate knowledge gained from laboratory work and animal models into novel therapies and drugs for human liver diseases.[34]

SPECIFIC MARKERS OF LIVER DEVELOPMENT

CLUSTER OF DIFFERENTIATION (CD) molecules and monoclonal antibodies (mAb) recognizing CD molecules have proved critical for identifying and characterizing hematopoietic cells, and more than 100 such molecules are routinely used as tools for tracking these cells in various situations. However, until recently, there were very few equivalent marker molecules specific for hepatic cells, making it difficult to distinguish and track hepatoblasts, bile duct cells and hepatocytes. The lack of such tools has hampered progress in the elucidation of liver development. The recent discovery of a battery collection spectrum of fetal liver-specific markers has facilitated detailed analyses of hepatic structural organization and the molecular mechanisms of liver formation. Several stages of liver organogenesis can now be characterized by their expression patterns of liver- and stage-specific genes. For example, α-fetoprotein (AFP) is an early fetal hepatic marker whose expression commences at E9 but decreases as liver development progresses.[35] In contrast, the expression of albumin, the most abundant protein synthesized by hepatocytes, starts in fetal hepatocytes at E10 and reaches its maximal level in murine adult hepatocytes.[36,37]

A key marker of the earliest stages of liver formation may be Dlk/Pref-1, a member of the δ-like family of cell surface transmembrane proteins. Use of the signal sequence trap method has shown that Dlk is strongly expressed in fetal liver between E12.5 and E16.5, specifically in highly proliferative hepatoblasts.[38] Dlk expression is then downregulated later during gestation and is absent from neonatal liver. Anti-Dlk antibodies have been generated and proven useful for the detection and isolation of primary hepatoblasts.[39] However, Dlk-deficient mice are viable without any apparent defects in liver formation or hematopoiesis,[40] making the exact role of Dlk in liver development unclear.

Our group has identified additional hepatic markers by preparing mAb specific for murine fetal livers and characterizing their binding to paraffin sections of mouse embryos at E11.5.[41] For example, the anti-Liv2 mAb binds specifically to hepatoblasts at E9.5–12.5. Although the Liv2 antigen has yet to be identified, it is clear that, unlike other common fetal hepatic markers such as AFP or albumin, Liv2 is not a diffusible serum protein and appears to be membrane-associated. We have found the anti-Liv2 mAb to be a useful tool for identifying murine hepatoblasts.[42–44]

Another example of a helpful mAb to come out of our studies is the anti-Liv8 mAb, which specifically recognizes the Liv8 antigen present in murine fetal livers at E11.5. Our initial studies showed that Liv8 is a cell surface molecule expressed by hematopoietic cells in both fetal liver and adult mouse bone marrow.[45,46] Subsequently, we have found that Liv8 is also transiently expressed by hepatoblasts at E11.5. Using protein purification and mass spectrometry, we have identified Liv8 as the CD44 protein. Interestingly, the expression of Liv8/CD44 in fetal liver is completely lost in *AML1*$^{-/-}$ murine embryos, which lack definitive hematopoiesis. These results show that hepatoblasts change from Liv8/CD44-negative to Liv8/CD44-positive status in a hematopoiesis-dependent manner by E11.5, and indicate that Liv8/CD44 expression is an important link between hematopoiesis and hepatogenesis during fetal liver development (Fig. 7).[47]

CD44 is the major receptor for hyaluronic acid (HA), a component of the extracellular matrix (ECM).[48] In addition to this adhesion function, CD44 has been identified as an intracellular signal transmitter, a growth factor presentation molecule, and a shaper of the ECM.[49] CD44 can be cleaved within its transmembrane domain such that its cytoplasmic tail is released into the cytoplasm. The CD44 cytoplasmic tail can then translocate to the nucleus, where it functions as a transcriptional activator. It remains unclear whether Liv8/CD44 itself transmits signals that control cellular proliferation and differentiation, or whether downstream intermediary molecules are involved. CD44 has also been reported to act as a linker that connects membrane-type 1 matrix metalloproteinase (MT1-MMP), which degrades ECM barriers during cancer invasion, to the actin cytoskeleton, and to play a role in directing MT1-MMP to the migration front. These data suggest that Liv8/CD44 may also contribute to the ECM reconstruction that is needed to create a niche in the fetal liver for incoming hematopoietic progenitors.

Kon *et al.* have shown that CD44 is a specific marker of "small hepatocytes", which are hepatic progenitor cells in adult liver.[50,51] Both *in vitro* and *in vivo*, CD44 expression is upregulated at the time small hepatocytes start to proliferate and differentiate. We have preliminary data suggesting that HA is also important for the proliferation of small hepatocytes, but that this mol-

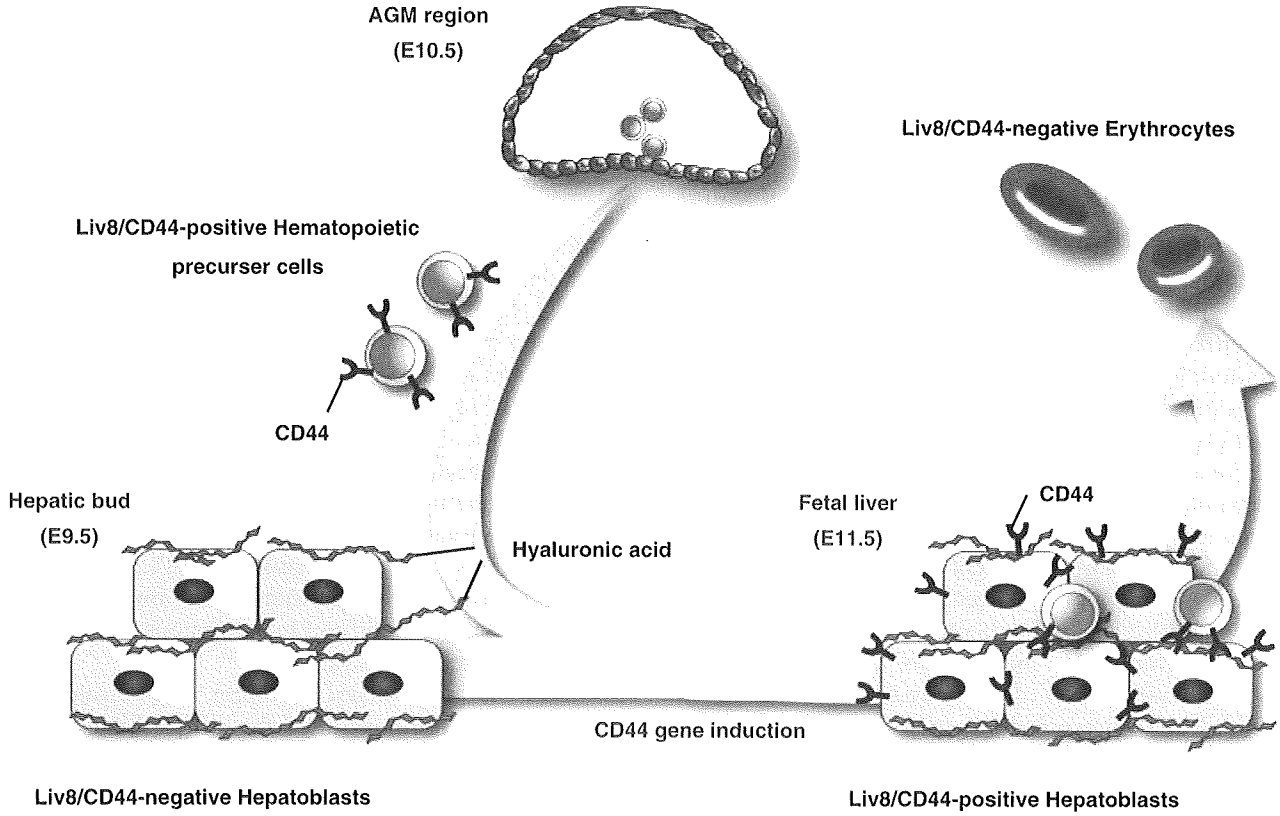

Figure 7 Liv8/CD44 function in fetal liver development. Hepatoblasts derived from the aorta–gonad–mesonephros (AGM) region emerge as Liv8/CD44-negative cells that populate the hepatic bud at embryonic day 9.5 (E9.5). These cells then become CD44-positive in a hematopoiesis-dependent manner at E11.5 and form a niche in the fetal liver that can accommodate an influx of Liv8/CD44-positive hematopoietic precursors. CD44 is thus an important link between hematopoiesis and hepatogenesis during fetal liver development.

ecule maintains these cells in their less-differentiated state. Therefore, it is possible that Liv8/CD44 plays an important role in the proliferation and/or differentiation of hepatic progenitor cells in both the embryo and the adult.

CONCLUSION

STUDIES OF MODEL organisms have revealed much about the molecular and cellular mechanisms of hepatogenesis. Traditional methods have focused on the genetic manipulation of rodents such as rats and mice but the more recent exploitation of lower organisms such as zebrafish and medaka has also provided much new information on liver formation and functions. In addition, the isolation of molecular markers and mAb specific for all stages of liver development is well underway and should aid future analyses. The knowledge gained from examining these markers and model organisms at the molecular level may contribute to progress in studies of liver biology and the treatment of liver disease.

ACKNOWLEDGMENTS

WE ARE GRATEFUL to Drs Isao Sakaida and Shuji Terai for critical reading and helpful discussions.

REFERENCES

1 Zaret KS. Regulatory phases of early liver development: paradigms of organogenesis. *Nat Rev Genet* 2002; **3**: 499–512.
2 Zaret KS, Grompe M. Generation and regeneration of cells of the liver and pancreas. *Science* 2008; **5** (322): 1490–4.

3 Zaret KS. Genetic programming of liver and pancreas progenitors: lessons for stem-cell differentiation. *Nat Rev Genet* 2008; **9**: 329–40.
4 Jung J, Zheng M, Goldfarb M, Zaret KS. Initiation of mammalian liver development from endoderm by fibroblast growth factors. *Science* 1999; **18** (284): 1998–2003.
5 Douarin NM. An experimental analysis of liver development. *Med Biol* 1975; **53**: 427–55.
6 Houssaint E. Differentiation of the mouse hepatic primordium. I. An analysis of tissue interactions in hepatocyte differentiation. *Cell Differ* 1980; **9**: 269–79.
7 Rossi JM, Dunn NR, Hogan BL, Zaret KS. Distinct mesodermal signals, including BMPs from the septum transversum mesenchyme, are required in combination for hepatogenesis from the endoderm. *Genes Dev* 2001; **1**: 1998–2009.
8 Bort R, Martinez-Barbera JP, Beddington RS, Zaret KS. Hex homeobox gene-dependent tissue positioning is required for organogenesis of the ventral pancreas. *Development* 2004; **131**: 797–806.
9 Martinez Barbera JP, Clements M, Thomas P *et al.* The homeobox gene Hex is required in definitive endodermal tissues for normal forebrain, liver and thyroid formation. *Development* 2000; **127**: 2433–45.
10 Thomas PQ, Brown A, Beddington RS. Hex: a homeobox gene revealing peri-implantation asymmetry in the mouse embryo and an early transient marker of endothelial cell precursors. *Development* 1998; **125**: 85–94.
11 Hunter MP, Wilson CM, Jiang X *et al.* The homeobox gene Hhex is essential for proper hepatoblast differentiation and bile duct morphogenesis. *Dev Biol* 2007; **15** (308): 355–67.
12 Beg AA, Sha WC, Bronson RT, Ghosh S, Baltimore D. Embryonic lethality and liver degeneration in mice lacking the RelA component of NF-kappa B. *Nature* 1995; **13** (376): 167–70.
13 Li Q, Van Antwerp D, Mercurio F, Lee KF, Verma IM. Severe liver degeneration in mice lacking the IkappaB kinase 2 gene. *Science* 1999; **9** (284): 321–5.
14 Li ZW, Chu W, Hu Y *et al.* The IKKbeta subunit of IkappaB kinase (IKK) is essential for nuclear factor kappaB activation and prevention of apoptosis. *J Exp Med* 1999; **7** (189): 1839–45.
15 Tanaka M, Fuentes ME, Yamaguchi K *et al.* Embryonic lethality, liver degeneration, and impaired NF-kappa B activation in IKK-beta-deficient mice. *Immun* 1999; **10**: 421–9.
16 Rudolph D, Yeh WC, Wakeham A *et al.* Severe liver degeneration and lack of NF-kappaB activation in NEMO/IKKgamma-deficient mice. *Genes Dev* 2000; **1** (14): 854–62.
17 Bonnard M, Mirtsos C, Suzuki S *et al.* Deficiency of T2K leads to apoptotic liver degeneration and impaired NF-kappaB-dependent gene transcription. *EMBO J* 2000; **15** (19): 4976–85.
18 Fruman DA, Mauvais-Jarvis F, Pollard DA *et al.* Hypoglycaemia, liver necrosis and perinatal death in mice lacking all isoforms of phosphoinositide 3-kinase p85 alpha. *Nat Genet* 2000; **26**: 379–82.
19 Ganiatsas S, Kwee L, Fujiwara Y *et al.* SEK1 deficiency reveals mitogen-activated protein kinase cascade crossregulation and leads to abnormal hepatogenesis. *Proc Natl Acad Sci USA* 1998; **9** (95): 6881–6.
20 Nishina H, Bachmann M, Oliveira-dos-Santos AJ *et al.* Impaired CD28-mediated interleukin 2 production and proliferation in stress kinase SAPK/ERK1 kinase (SEK1)/mitogen-activated protein kinase kinase 4 (MKK4)-deficient T lymphocytes. *J Exp Med* 1997; **15** (186): 941–53.
21 Nishina H, Fischer KD, Radvanyi L *et al.* Stress-signalling kinase Sek1 protects thymocytes from apoptosis mediated by CD95 and CD3. *Nature* 1997; **23** (385): 350–3.
22 Nishina H, Vaz C, Billia P *et al.* Defective liver formation and liver cell apoptosis in mice lacking the stress signaling kinase SEK1/MKK4. *Development* 1999; **126**: 505–16.
23 Yang D, Tournier C, Wysk M *et al.* Targeted disruption of the MKK4 gene causes embryonic death, inhibition of c-Jun NH2-terminal kinase activation, and defects in AP-1 transcriptional activity. *Proc Natl Acad Sci USA* 1997; **1** (94): 3004–9.
24 Hilberg F, Aguzzi A, Howells N, Wagner EF. c-jun is essential for normal mouse development and hepatogenesis. *Nature* 1993; **9** (365): 179–81.
25 Johnson RS, van Lingen B, Papaioannou VE, Spiegelman BM. A null mutation at the c-jun locus causes embryonic lethality and retarded cell growth in culture. *Genes Dev* 1993; **7**: 1309–17.
26 Wada T, Joza N, Cheng HY *et al.* MKK7 couples stress signalling to G2/M cell-cycle progression and cellular senescence. *Nat Cell Biol* 2004; **6**: 215–26.
27 Davenport TG, Jerome-Majewska LA, Papaioannou VE. Mammary gland, limb and yolk sac defects in mice lacking Tbx3, the gene mutated in human ulnar mammary syndrome. *Development* 2003; **130**: 2263–73.
28 Suzuki A, Sekiya S, Buscher D, Izpisua Belmonte JC, Taniguchi H. Tbx3 controls the fate of hepatic progenitor cells in liver development by suppressing $p19^{ARF}$ expression. *Development* 2008; **135**: 1589–95.
29 Zhao R, Duncan SA. Embryonic development of the liver. *Hepatology* 2005; **41**: 956–67.
30 Field HA, Ober EA, Roeser T, Stainier DY. Formation of the digestive system in zebrafish. I. Liver morphogenesis. *Dev Biol* 2003; **15** (253): 279–90.
31 Ober EA, Verkade H, Field HA, Stainier DY. Mesodermal Wnt2b signaling positively regulates liver specification. *Nature* 2006; **10** (442): 688–91.
32 Sakaguchi TF, Sadler KC, Crosnier C, Stainier DY. Endothelial signals modulate hepatocyte apicobasal polarization in zebrafish. *Curr Biol* 2008; **28** (18): 1565–71.

33 Watanabe T, Asaka S, Kitagawa D *et al.* Mutations affecting liver development and function in Medaka, Oryzias latipes, screened by multiple criteria. *Mech Dev* 2004; **121**: 791–802.
34 Matsumoto T, Terai S, Kuwashiro S *et al.* The Development of new drug screening system using steatohepatitis Medaka fish model induced by high fat diet. *Hepatology* 2007; **46** (4 Suppl 1): 756A.
35 Shiojiri N. Enzymo- and immunocytochemical analyses of the differentiation of liver cells in the prenatal mouse. *J Embryol Exp Morphol* 1981; **62**: 139–52.
36 Murakami T, Yasuda Y, Mita S *et al.* Prealbumin gene expression during mouse development studied by in situ hybridization. *Cell Differ* 1987; **22**: 1–9.
37 Tilghman SM, Belayew A. Transcriptional control of the murine albumin/alpha-fetoprotein locus during development. *Proc Natl Acad Sci USA* 1982; **79**: 5254–7.
38 Tanimizu N, Nishikawa M, Saito H, Tsujimura T, Miyajima A. Isolation of hepatoblasts based on the expression of Dlk/Pref-1. *J Cell Sci* 2003; **1** (116): 1775–86.
39 Tanimizu N, Tsujimura T, Takahide K, Kodama T, Nakamura K, Miyajima A. Expression of Dlk/Pref-1 defines a subpopulation in the oval cell compartment of rat liver. *Gene Expr Patterns* 2004; **5**: 209–18.
40 Moon YS, Smas CM, Lee K *et al.* Mice lacking paternally expressed Pref-1/Dlk1 display growth retardation and accelerated adiposity. *Mol Cell Biol* 2002; **22**: 5585–92.
41 Watanabe T, Nakagawa K, Ohata S *et al.* SEK1/MKK4-mediated SAPK/JNK signaling participates in embryonic hepatoblast proliferation via a pathway different from NF-kappaB-induced anti-apoptosis. *Dev Biol* 2002; **15** (250): 332–47.
42 Ishikawa T, Terai S, Urata Y *et al.* Fibroblast growth factor 2 facilitates the differentiation of transplanted bone marrow cells into hepatocytes. *Cell Tissue Res* 2006; **323**: 221–31.
43 Nierhoff D, Ogawa A, Oertel M, Chen YQ, Shafritz DA. Purification and characterization of mouse fetal liver epithelial cells with high in vivo repopulation capacity. *Hepatology* 2005; **42**: 130–9.
44 Suzuki T, Kanai Y, Hara T *et al.* Crucial role of the small GTPase ARF6 in hepatic cord formation during liver development. *Mol Cell Biol* 2006; **26**: 6149–56.
45 Sakaida I, Terai S, Yamamoto N *et al.* Transplantation of bone marrow cells reduces CCl4-induced liver fibrosis in mice. *Hepatology* 2004; **40**: 1304–11.
46 Yamamoto N, Terai S, Ohata S *et al.* A subpopulation of bone marrow cells depleted by a novel antibody, anti-Liv8, is useful for cell therapy to repair damaged liver. *Biochem Biophys Res Commun* 2004; **23** (313): 1110–8.
47 Ohata S, Nawa M, Kasama T *et al.* Hematopoiesis-dependent expression of CD44 in murine hepatic progenitor cells. *Biochem Biophys Res Commun* 2009; **20** (379): 817–23.
48 Aruffo A, Stamenkovic I, Melnick M, Underhill CB, Seed B. CD44 is the principal cell surface receptor for hyaluronate. *Cell* 1990; **29** (61): 1303–13.
49 Ponta H, Sherman L, Herrlich PA. CD44: from adhesion molecules to signaling regulators. *Nat Rev Mol Cell Biol* 2003; **4**: 33–45.
50 Kon J, Ooe H, Oshima H, Kikkawa Y, Mitaka T. Expression of CD44 in rat hepatic progenitor cells. *J Hepatol* 2006; **45**: 90–8.
51 Mitaka T, Mikami M, Sattler GL, Pitot HC, Mochizuki Y. Small cell colonies appear in the primary culture of adult rat hepatocytes in the presence of nicotinamide and epidermal growth factor. *Hepatology* 1992; **16**: 440–7.

BMC Research Notes

BioMed Central

Short Report

Open Access

Medaka: a promising model animal for comparative population genomics

Yoshifumi Matsumoto[†1,7], Hiroki Oota[*†1], Yoichi Asaoka[2], Hiroshi Nishina[2], Koji Watanabe[3], Janusz M Bujnicki[4,5,6], Shoji Oda[1], Shoji Kawamura[1] and Hiroshi Mitani[*1]

Address: [1]Department of Integrated Biosciences, Graduate School of Frontier Sciences, University of Tokyo, Tokyo, Japan, [2]Department of Developmental and Regenerative Biology, Medical Research Institute, Tokyo Medical and Dental University, Tokyo, Japan, [3]FUJIYA CO., LTD., Kanagawa, Japan, [4]Department of Medical Genome Sciences, Graduate School of Frontier Sciences, University of Tokyo, Tokyo, Japan, [5]International Institute of Molecular and Cell Biology, Warsaw, Poland, [6]Institute of Molecular Biology and Biotechnology, Faculty of Biology, Adam Mickiewicz University, Poznan, Poland and [7]Laboratory for Behavioral and Developmental Disorders, Brain Science Institute, RIKEN, Saitama, Japan

Email: Yoshifumi Matsumoto - miraihe08@brain.riken.jp; Hiroki Oota* - hiroki_oota@k.u-tokyo.ac.jp; Yoichi Asaoka - y-asaoka.dbio@mri.tmd.ac.jp; Hiroshi Nishina - nishina.dbio@mri.tmd.ac.jp; Koji Watanabe - peko-poko-fujiya@ab.inbox.ne.jp; Janusz M Bujnicki - iamb@genesilico.pl; Shoji Oda - odasho@k.u-tokyo.ac.jp; Shoji Kawamura - kawamura@k.u-tokyo.ac.jp; Hiroshi Mitani* - mitani@k.u-tokyo.ac.jp

* Corresponding authors †Equal contributors

Published: 10 May 2009

BMC Research Notes 2009, **2**:88 doi:10.1186/1756-0500-2-88

Received: 25 March 2009
Accepted: 10 May 2009

This article is available from: http://www.biomedcentral.com/1756-0500/2/88

Abstract

Background: Within-species genome diversity has been best studied in humans. The international HapMap project has revealed a tremendous amount of single-nucleotide polymorphisms (SNPs) among humans, many of which show signals of positive selection during human evolution. In most of the cases, however, functional differences between the alleles remain experimentally unverified due to the inherent difficulty of human genetic studies. It would therefore be highly useful to have a vertebrate model with the following characteristics: (1) high within-species genetic diversity, (2) a variety of gene-manipulation protocols already developed, and (3) a completely sequenced genome. Medaka (*Oryzias latipes*) and its congeneric species, tiny fresh-water teleosts distributed broadly in East and Southeast Asia, meet these criteria.

Findings: Using *Oryzias* species from 27 local populations, we conducted a simple screening of nonsynonymous SNPs for 11 genes with apparent orthology between medaka and humans. We found medaka SNPs for which the same sites in human orthologs are known to be highly differentiated among the HapMap populations. Importantly, some of these SNPs show signals of positive selection.

Conclusion: These results indicate that medaka is a promising model system for comparative population genomics exploring the functional and adaptive significance of allelic differentiations.

Background

The accumulation of human genetic polymorphism data provided by sources such as the international HapMap project [1,2] has revealed a number of SNP sites with markedly different allele frequencies among human populations. Such data make systematic searches for disease-causing or drug-responsive genomic regions possible [3,4], and the accumulated SNP data can also provide compelling evidence of positive selection during human evolution [5,6]. An inevitable issue, however, is that mutagenesis and/or crossing-over experiments to elucidate functional differences between alleles at these polymorphic sites are practically impossible in humans. A vertebrate model animal with a broad geographic distribution and documented high genetic polymorphism could serve as a "natural library" of genetic variation in humans for orthologous genes that could be under similar selective pressures.

The medaka (*Oryzias latipes*) is a notable candidate for such a model animal. This small freshwater fish is found in East Asia with closely related congeneric species broadly distributed throughout Southeast Asia, and it has a long history of use as an experimental animal since the early 20th century. A number of inbred medaka strains have been established, and transgenesis and mutagenesis protocols have been developed, suggesting that medaka has great potential for use in systematic genetic analyses [7-10]. Medaka genome sequences are also available [11]. The greatest advantage of using medaka is its enormous genetic diversity compared to the other fish models (zebrafish, pufferfish, etc.), with the average nucleotide difference of 3.4% between two inbred medaka strains being the highest among any vertebrates thus far documented [11]. In this study, our purpose is to assess the validity of medaka as a useful resource of comparative population genomics.

Methods

Medaka strains

Japanese medaka (*Oryzias latipes*) populations consist of four geographical populations. We selected 24 wild-type strains from the Japanese medaka (see Additional file 1) and three closely related congeneric species (*O. curvinotus*, *O. luzonensis* and *O. celebensis*; see Additional file 2). We also examined an inbred strain (Hd-rR) of Southern Japanese origin.

PCR-direct sequence, mRNA extraction and cDNA sequence

We selected 11 genes for the screening of madaka SNPs (Table 1). The flow chart of the target gene selection is shown in Figure 1a. The PCR primers were designed on the basis of the medaka genomic sequences [11] corresponding to those of humans where high-F_{st} SNPs are found (Fig. 1b). The PCR performed using genomic DNA extracted from medaka fins or bodys as template. To isolate entire *oRTTN* sequences, mRNAs were prepared from the embryos of seven strains, because we had already confirmed by in situ hybridization that *oRTTN* was expressed in early developmental stages. *oRTTN* genes were PCR amplified with primer pairs designed using the *oRTTN* sequence predicted from the medaka genome project (Hd-rR strain)[11]. The PCR products were directly sequenced using an ABI PRISM 3130-Avant Genetic Analyzer (Applied Biosystems Japan, Tokyo, Japan) and a total of ~340 kb of DNA sequences were obtained. The primer sequences and the determined sequences have been deposited in the international GenBank/DDBJ/EMBL nucleotide sequence database [accession nos. AB435679 - AB435956]. The thermocycling conditions are available on request.

Statistical and phylogenetic analysis

Nucleotide sequences were aligned using CLUSTALW [12]. The pairwise *dN* and *dS* values among strains of 11 genes were calculated by DnaSP Software (version 4.0) according to the Nei-Gojobori method [13]. Insertions and deletions (indels) were excluded from analysis. For the entire nucleotide sequence of *RTTN*, the *d*N-*d*S and *p*-values were calculated by MEGA 4 [14] according to the Nei-Gojobori method with statistical significance tested by Z-tests.

Protein structure prediction

The GeneSilico metaserver [15] was used to predict protein secondary structure and order/disorder, and to carry out fold-recognition (i.e. match the query sequence with structurally characterized templates). Potential phosphorylation sites were predicted using a semi-independent component of the metaserver available at the URL http://genesilico.pl/Phosphoserver/. For the THEA2 protein, the metaserver indicated very high similarity (PCONS score 3.28) of residues 1-360 (human numbering) to known Acyl-CoA hydrolase structures (e.g. 2gvh in the Protein Data Bank) and high similarity of residues 360-607 (PCONS score 2.00) to lipid transfer proteins from the STAR family (e.g. 1ln1 in the PDB). Long regions of intrinsic conformational disorder were predicted for loops connecting structural domains (around residues 160-200 and 340-370). For the RTTN protein, the metaserver identified the α-helical armadillo domain of β-catenin (1i7w in Protein Data Bank) as the best modeling template, in particular for residues 1-120, with a high confidence score (PCONS score 1.67). Long regions of structural disorder, devoid of secondary and tertiary structure, were predicted for residues 120-160 and 280-370. Three-dimensional structural models of the ordered (i.e. stably folded) parts of THEA2 and RTTN proteins were generated and optimized using the FRankenstein's Monster method

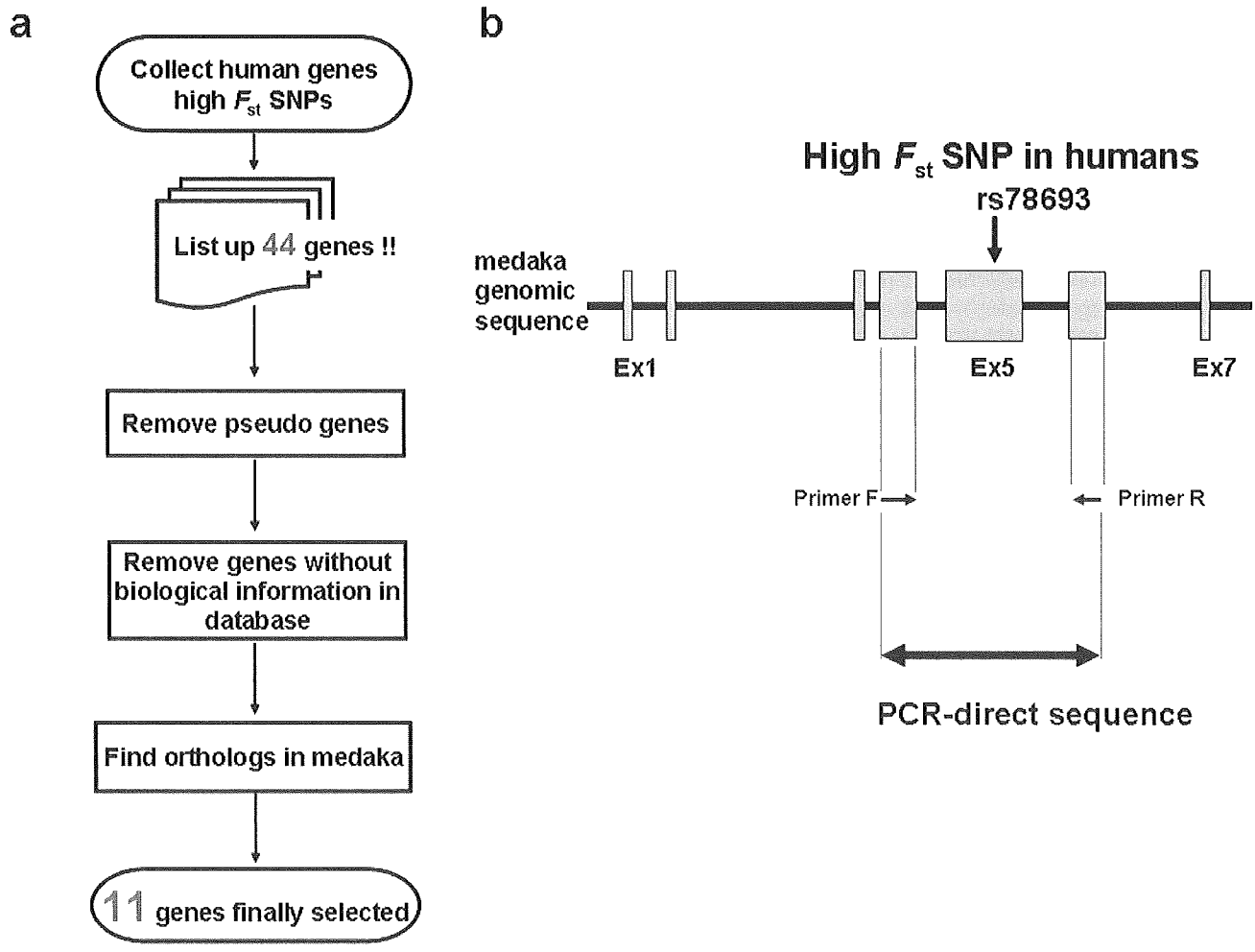

Figure 1

(a) Flow chart of targeted gene selection, and (b) a schema of the SNP screening method. We first focused on 44 genes with allele frequencies highly differentiated among human populations, including the 27 genes listed in Table nine of the first HapMap paper [1] based on high F_{st} values for nonsynonymous SNPs and the 17 genes listed in Table S4 of Sabeti et al. (2006) in the category "population differentiation." A SNP site with a F_{st} value higher than the genome average represents higher population differentiation at this site [26], possibly driven by natural selection [27-30]. Secondly, from the 44 genes, we removed pseudogenes, genes with unclear annotation and genes without biological information in the database. Thirdly, we chose genes for which only a single gene was assigned as an ortholog in the medaka genome by searching the Ensembl database http://www.ensembl.org/index.html. After applying these selection criteria, 11 genes were subjected to the SNP screening (Table 1).

[16]. The final models were evaluated as good quality by the PROQ server [17]. The models were expected to exhibit a root mean square deviation to the true structures in the order of 2–4 Å, suggesting that they are sufficiently reliable to make functional predictions at the level of individual amino acid residues. The atomic details of these models, however, must be taken with a grain of salt.

Results and discussion

Of the 11 genes, we found that medaka *THEA2* (*BFIT2*) contained a nonsynonymous SNP at the exactly same site where a high F_{st} is observed in humans (rs1702003 in exon 6: see the HapMap database; Fig. 2). *THEA2* is known to be a temperature responsive gene, and it is expressed in brown adipose tissue (BAT) in response to cold stress in mice [18]. The genotype frequencies at rs1702003 are 98.3% G/G and 1.7% G/A in Europeans and 100% A/A in East Asians and Africans. This could suggest that the European-specific allele of the cold-inducible gene is an adaptation of Europeans to the cold environment around 40,000 years ago when early modern humans expanded to Europe. Interestingly, only Philip-

Table 1: The 11 genes examined in this study

Gene	Gene ontology "biological process" annotation
ALDH2	alcohol metabolic process
EDAR	I-kappaB kinase/NF-kappaB cascade
F2	coagulation factor II
GRK4	regulation of G-protein coupled receptor protein signaling pathway
LCT	Lactase
RTTN	required for axial rotation and left-right specification
SLC24A5	solute carrier family 24, member 5
SLC30A9	solute carrier family 30 (zinc transporter), member 9
SLC45A2	solute carrier family 45, member 2
LWS	opsin 1 (cone pigments), long-wave-sensitive (color blindness, protan)
THEA2	response to temperature stimulus

Figure 2
Nucleotide (upper) and amino acid (lower) sequence alignments of *THEA2*. Hd-rR is the inbred strain derived from the southern Japanese population for which the complete genome sequence has been determined [11]. All three (Hd-rR, Northern Japanese and East Korea) are *Oryzias latipes*. The others are closely related species.

pine medaka (*Oryzias luzonensis*), inhabiting a warmer environment, has a different allele from the other *Oryzias* species. While in *situ* hybridization showed *THEA2* is expressed ubiquitously in medaka embryos, RT-PCR indicated greater *THEA2* expression in the brown tissue homologous to mammalian BAT than in the other tissues in adult medaka (data not shown). In the structural predictions for the THEA2, we found that the two SNPs indicated for the human and medaka proteins are located at the junction between the Acyl-CoA hydrolase structural domains in a loop predicted to be highly flexible. There, a G-D (in humans) or L-P change (in medaka) is likely to affect the dynamics of the protein chain and influence (1) the interaction between domains and/or (2) the transmission of conformational changes. We speculate that the amino acid change that affects protein flexibility may be related to temperature adaptation.

For another gene, *RTTN*, we found even more remarkable regional differentiation. The phylogenetic network adding nine individuals from the northern Japanese population and one southern Japanese population indicates the nucleotide changes in the *RTTN* gene among geographical populations; each population forms a separate cluster and is separated by unique amino acid changes (Fig. 3). According to bioinformatic predictions, the RTTN protein is comprised of armadillo-like repeats separated in a few places by disordered loops (Fig. 4). A78 is partially buried and its substitution may destabilize the protein structure. S92 is located on the surface and is predicted to be phosphorylated; hence, its substitution may affect structure

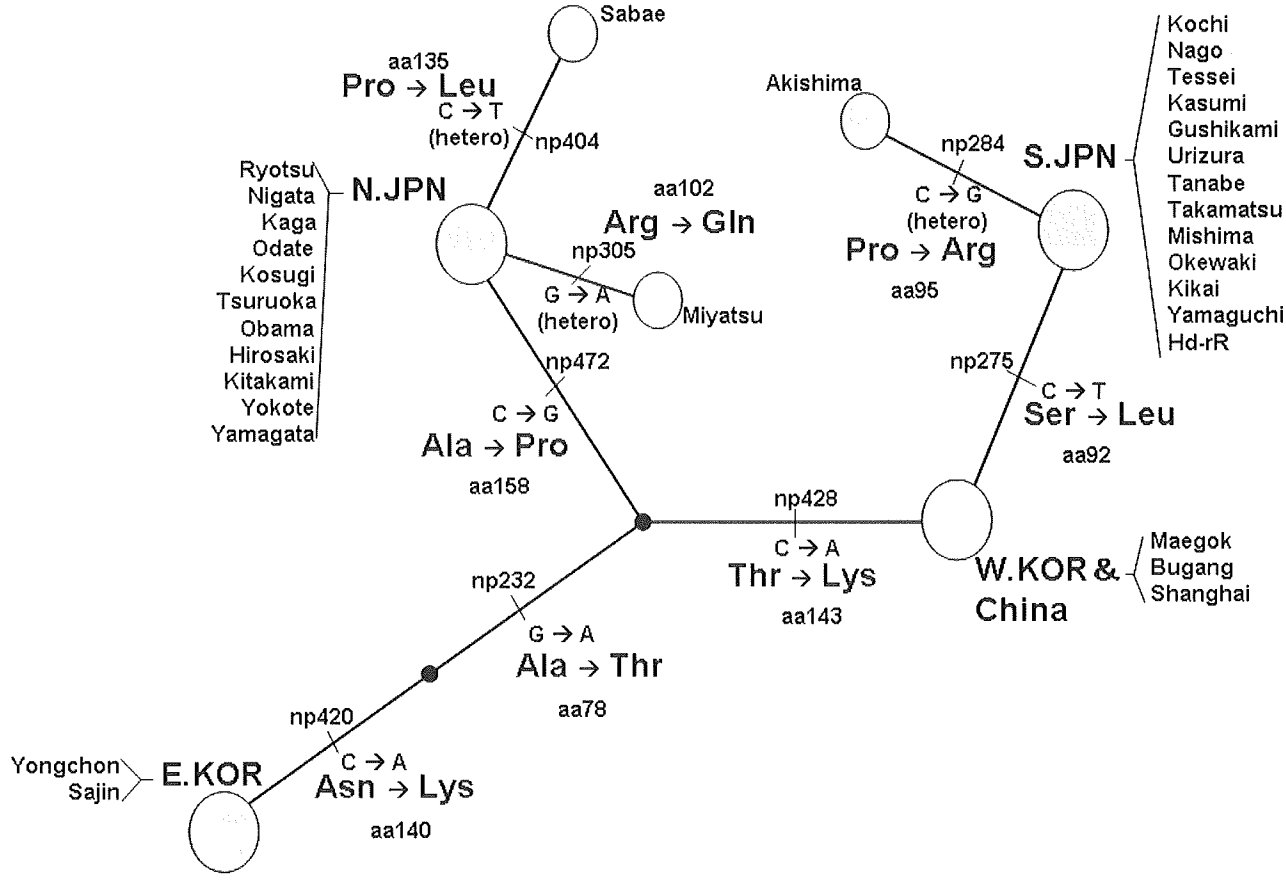

Figure 3
Phylogenetic network of *RTTN* based on nucleotide sequences from exons 3 + 4 (271 bp). The circle represents geographical regional strains (N.JPN: northern Japanese population; S.JPN: southern Japanese population; W.KOR: western Korean; E.KOR: eastern Korean). "np" represents the nucleotide position number. The "aa" numbers are the amino acid sequence positions.

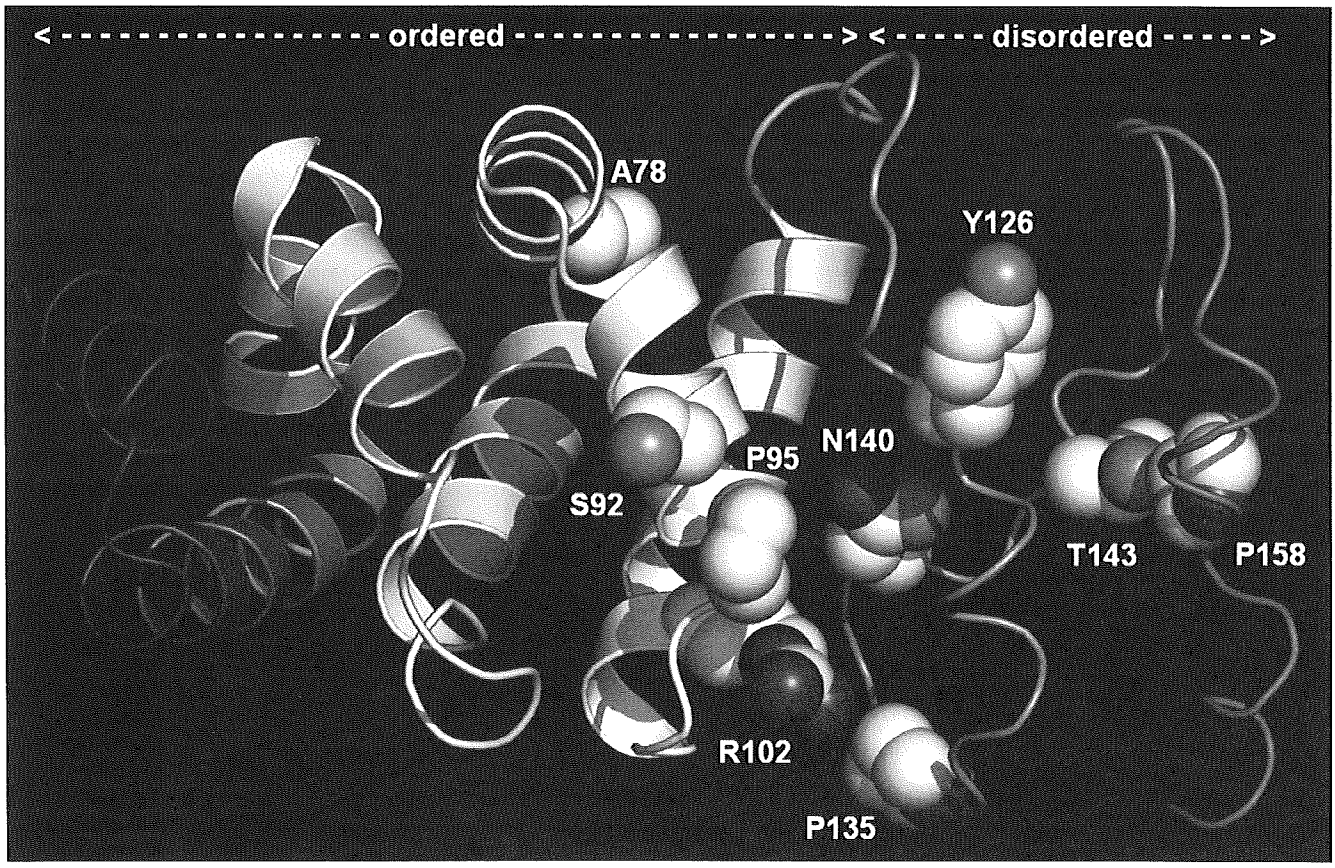

Figure 4
Structure prediction for *RTTN*: a well-folded globular part (armadillo-like repeats, aa 1 – 120) and an unstructured linker (aa 121 – 166). The protein chain is colored from blue (N-terminus) to red (C-terminus). α-helices are shown as ribbons. Side chains of residues substituted because of SNPs are shown in the "spacefill" representation and labeled; C, O, and N atoms are shown in gray, red, and blue, respectively. The positions of amino acid changes and the medaka populations sharing these changes are as follows: aa78, Thr: E.KOR, Ala: Others; aa92, Ser: S.JPN, Leu: Others; aa95, Arg: Akishima, Pro: Others; aa102, Gln: Miyatsu, Arg: Others, aa135, Leu: Sabae, Pro: Others; aa140, Lys: E.KOR, Asn: Others; aa143, Thr: E.KOR, N.JPN, Lys: W.KOR & China, and S.JPN; aa158, Ala: N.JPN, Pro: Others.

and/or function by removing a site of posttranslational modification. N140, T143, and P158 are in the disordered loop. Substituting P158 with A may increase the flexibility of the main chain, the introduction of K140 and K143 may increase the entropy of the side chain, and substitution of T143 (predicted to be phosphorylated) may remove a site of posttranslational modification. Thus, substitutions of all these residues are predicted to influence the dynamics of the loop and thus its ability to bind to other molecules or to respond to changes in the environment.

To gain further insight into whether natural selection is involved in the observed nucleotide variations, we plotted the average number of nonsynonymous nucleotide differences per number of nonsynonymous sites (d_N) against the average number of synonymous nucleotide differences per number of synonymous sites (d_S) estimated for the 11 genes among the 27 medaka strains (Fig. 5). Seven of the 11 genes including *THEA2* showed an average d_N/d_S of less than 1, suggesting that the seven genes are under purifying selection. In *RTTN*, in contrast, there are only nonsynonymous differences in the genomic regions examined (exons 3 and 4: 271 bp in total); in more than half of the population pairs, the d_N/d_S ratios are significantly greater than 1 (Z-test; $p < 0.05$). The d_N/d_S ratios of the *LTC* and the *GRK4* genes are also greater than 1, but these are not statistically significant at 5% level for any pair. We have sequenced the entire *RTTN* cDNA for seven individual medaka from five geographical populations. Although there are synonymous variations in the other exons, the d_N/d_S ratios are overall greater than 1, and in

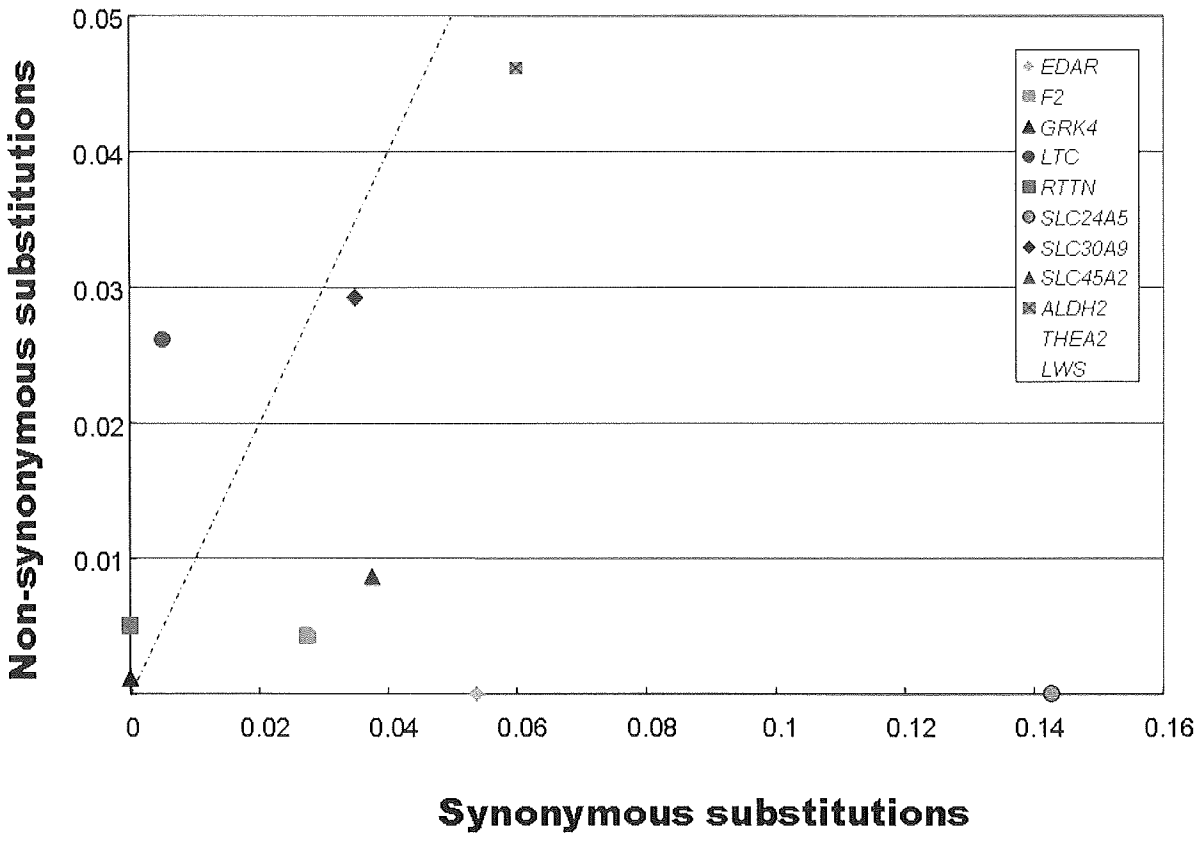

Figure 5
Synonymous (X axis) and nonsynonymous (Y axis) substitution ratios estimated by the Nei – Gojobori method. A *d*N/*d*S ratio significantly greater than 1 is a convincing indicator of positive selection.

Table 2: The *d*N - *d*S values (upper diagonal) and the significance (lower diagonal) based on *RTTN* cDNA (5.8 kb) sequences

	Population samples	Nigata	Iwaki	Mishima	Nago	Shanghai	Maegok	Yongchon
N.JPN	Nigata		1.622	1.712	1.685	1.116	1.835	1.87
	Iwaki	0.054		2.988	1.674	0.847	1.567	1.077
S.JPN	Mishima	0.045	0.002*		2.005	0.91	1.507	1.072
	Nago	0.047*	0.048*	0.024*		1.009	1.886	0.876
China	Shanghai	0.133	0.199	0.182	0.157		0.549	1.218
W.KOR	Maegok	0.035*	0.06	0.067	0.031*	0.292		2.103
E.KOR	Yongchon	0.032*	0.142	0.143	0.191	0.113	0.019*	

* represents 5% level significance of *p*-value in Z-test. "N. JPN" and "S.JPN" represent North and South Japan medaka, respectively. "W.KOR" and "E.KOR" represent West and East Korea medaka, respectively

nine of the 21 pairs they are statistically significant ($p < 0.05$; Table 2). These results suggest that *RTTN* is under positive selection in medaka.

Although its exact function is not known, *RTTN* is reported to be involved in determining the rotation of the body axis and the left-right asymmetry of internal organs during the embryonic development of mice [19]. The conspicuous differentiation of *RTTN* alleles among human populations also suggests differential natural selection acting on different populations: at a nonsynonymous SNP site (rs3911730) in the *RTTN* exon 3, the A/A genotype occurs in 90% of Africans, 2% of Europeans and is absent in Asians, while the C/C genotype occurs in 3% of Africans, 80% of Europeans and 100% of Asians.

Previous studies have reported that genes identified in fish through "forward genetic" analysis of phenotypic mutants are involved in forming variations of related phenotypes in humans, e.g. of skin pigmentation [20-24] and epithelial development [25]. Our approach in this study is an extension of these previous studies, as a form of "reverse genetics" of genes that show, as a signature of natural selection acting on them, a prominent level of diversification in the allele frequency among populations with different ecological histories in both fish and humans. We found that out of 11 genes in our analysis, the medaka *THEA2* gene has a nonsynonymous polymorphic site at exactly the same position as its ortholog in humans, and the *RTTN* gene shows signs of population differentiation that can be explained plausibly by natural selection. The aim of our analysis is not to demonstrate evidence of natural selection in medaka, but to indicate that medaka is a marvelous resource as a "natural library" of genetic diversity, and this approach is efficient enough to find candidate genes targeted by natural selection in both humans and medaka. The exact function of the genes and the exact nature of the functional differences between alleles can be studied more feasibly in medaka, where crossing experiments between different genotypes of interest and transgenic techniques have already been established [7,8]. This method can be applied to any polymorphic gene in humans, and larger-scale and more systematic screening of orthologous gene polymorphisms in medaka will find various target genes for further functional analyses. As the medaka has been widely used for carcinogenesis and ecotoxicological studies [7], for example, in screening for genetic variants concerning medaka carcinogenesis and ecotoxins, it could also be used for testing variations in drug response in humans. Thus, we conclude that the medaka is a good vertebrate model of the functional diversity caused by human DNA polymorphisms that have been identified by recent resequencing and typing efforts.

Authors' contributions

HO conceived, and SK and HM formed the project. SO and HM provided the medaka resources. HO, YM, and HM designed the experiments. KW and YM performed PCRs and sequencing. For *THEA2* and *RTTN*, YM performed the RT-PCRs and cDNA sequencing, YA and HN performed WISH. JMB performed protein structure predictions. HO and YM analyzed the data and wrote the paper. All authors read and approved the final manuscript.

Additional material

Additional file 1

Sampling map of regional strains for Oryzias latipes. *Four strains (Nigata, Ryotsu, Kaga and Odate) are from the Northern Japanese population, and 15 strains (Tanabe, Takamatsu, Tessei, Kasumi, Uridura, Iwaki, Mishima, Hagi, Okewaki, Kikai, Nago, Kochi, Yamaguchi, Akishima and Gushikami) are from the Southern Japanese population. Two strains (Yongchon and Sajin) are from the Eastern Korean population, and three strains (Maegok, Bugang and Shanghai) are from Western Korean and Chinese populations. For the* RTTN *gene, we examined nine additional individuals from seven wild strains (Kosugi, Tsuruoka, Obama, Hirosaki, Kamikita, Yokote, Yamagata) from the Northern Japanese population.*
Click here for file
[http://www.biomedcentral.com/content/supplementary/1756-0500-2-88-S1.tiff]

Additional file 2

Sampling map of regional strains for closely related species.
Click here for file
[http://www.biomedcentral.com/content/supplementary/1756-0500-2-88-S2.tiff]

Acknowledgements

This work was supported by a Grant-in-Aid for Scientific Research (A) from the Japan Society for the Promotion of Science (JSPS) (19207018) to SK, by a Grant-in-Aid for Scientific Research (C) from JSPS (19570226) to HO, and by a Grant-in-Aid for Scientific Research in the Priority Area "Comparative Genomics" (#015) from the Ministry of Education, Culture, Sports, Science and Technology of Japan (MEXT) to HM. We thank Professor Emeritus Akihiro Shima and Dr. Atsuko Shimada (the University of Tokyo) for their efforts on keeping medaka stocks from wild populations.

References

1. The_international_HapMap_consortium: **A haplotype map of the human genome.** *Nature* 2005, **437**:1299-1320.
2. Frazer KA, Ballinger DG, Cox DR, Hinds DA, Stuve LL, Gibbs RA, Belmont JW, Boudreau A, Hardenbol P, Leal SM, *et al.*: **A second generation human haplotype map of over 3.1 million SNPs.** *Nature* 2007, **449**:851-861.
3. Conrad DF, Jakobsson M, Coop G, Wen X, Wall JD, Rosenberg NA, Pritchard JK: **A worldwide survey of haplotype variation and linkage disequilibrium in the human genome.** *Nat Genet* 2006, **38**:1251-1260.
4. McVean G, Spencer CC, Chaix R: **Perspectives on human genetic variation from the HapMap Project.** *PLoS Genet* 2005, **1**:e54.
5. Voight BF, Kudaravalli S, Wen X, Pritchard JK: **A map of recent positive selection in the human genome.** *PLoS Biol* 2006, **4**:e72.

6. Williamson SH, Hubisz MJ, Clark AG, Payseur BA, Bustamante CD, Nielsen R: **Localizing recent adaptive evolution in the human genome.** *PLoS Genet* 2007, **3**:e90.
7. Wittbrodt J, Shima A, Schartl M: **Medaka – a model organism from the far East.** *Nat Rev Genet* 2002, **3**:53-64.
8. Shima A, Mitani H: **Medaka as a research organism: past, present and future.** *Mech Dev* 2004, **121**:599-604.
9. Naruse K, Hori H, Shimizu N, Kohara Y, Takeda H: **Medaka genomics: a bridge between mutant phenotype and gene function.** *Mech Dev* 2004, **121**:619-628.
10. Matsumoto Y, Fukamachi S, Mitani H, Kawamura S: **Functional characterization of visual opsin repertoire in Medaka (Oryzias latipes).** *Gene* 2006, **371**:268-278.
11. Kasahara M, Naruse K, Sasaki S, Nakatani Y, Qu W, Ahsan B, Yamada T, Nagayasu Y, Doi K, Kasai Y, *et al.*: **The medaka draft genome and insights into vertebrate genome evolution.** *Nature* 2007, **447**:714-719.
12. Thompson JD, Higgins DG, Gibson TJ: **CLUSTAL W: improving the sensitivity of progressive multiple sequence alignment through sequence weighting, position-specific gap penalties and weight matrix choice.** *Nucleic Acids Res* 1994, **22**:4673-4680.
13. Nei M, Gojobori T: **Simple methods for estimating the numbers of synonymous and nonsynonymous nucleotide substitutions.** *Mol Biol Evol* 1986, **3**:418-426.
14. Tamura K, Dudley J, Nei M, Kumar S: **MEGA4: Molecular Evolutionary Genetics Analysis (MEGA) software version 4.0.** *Mol Biol Evol* 2007, **24**:1596-1599.
15. Kurowski MA, Bujnicki JM: **GeneSilico protein structure prediction meta-server.** *Nucleic Acids Res* 2003, **31**:3305-3307.
16. Kosinski J, Cymerman IA, Feder M, Kurowski MA, Sasin JM, Bujnicki JM: **A "FRankenstein's monster" approach to comparative modeling: merging the finest fragments of Fold-Recognition models and iterative model refinement aided by 3D structure evaluation.** *Proteins* 2003, **53(Suppl 6)**:369-379.
17. Wallner B, Elofsson A: **Identification of correct regions in protein models using structural, alignment, and consensus information.** *Protein Sci* 2006, **15**:900-913.
18. Adams SH, Chui C, Schilbach SL, Yu XX, Goddard AD, Grimaldi JC, Lee J, Dowd P, Colman S, Lewin DA: **BFIT, a unique acyl-CoA thioesterase induced in thermogenic brown adipose tissue: cloning, organization of the human gene and assessment of a potential link to obesity.** *Biochem J* 2001, **360**:135-142.
19. Faisst AM, Alvarez-Bolado G, Treichel D, Gruss P: **Rotatin is a novel gene required for axial rotation and left-right specification in mouse embryos.** *Mech Dev* 2002, **113**:15-28.
20. Fukamachi S, Shimada A, Shima A: **Mutations in the gene encoding B, a novel transporter protein, reduce melanin content in medaka.** *Nat Genet* 2001, **28**:381-385.
21. Lamason RL, Mohideen MA, Mest JR, Wong AC, Norton HL, Aros MC, Jurynec MJ, Mao X, Humphreville VR, Humbert JE, *et al.*: **SLC24A5, a putative cation exchanger, affects pigmentation in zebrafish and humans.** *Science* 2005, **310**:1782-1786.
22. Nakayama K, Fukamachi S, Kimura H, Koda Y, Soemantri A, Ishida T: **Distinctive distribution of AIM1 polymorphism among major human populations with different skin color.** *J Hum Genet* 2002, **47**:92-94.
23. Fukamachi S, Kinoshita M, Tsujimura T, Shimada A, Oda S, Shima A, Meyer A, Kawamura S, Mitani H: **Rescue From Oculocutaneous Albinism Type 4 Using Medaka slc45a2 cDNA Driven by Its Own Promoter.** *Genetics* 2008, **178**:761-769.
24. Miller CT, Beleza S, Pollen AA, Schluter D, Kittles RA, Shriver MD, Kingsley DM: **cis-Regulatory changes in Kit ligand expression and parallel evolution of pigmentation in sticklebacks and humans.** *Cell* 2007, **131**:1179-1189.
25. Kondo S, Kuwahara Y, Kondo M, Naruse K, Mitani H, Wakamatsu Y, Ozato K, Asakawa S, Shimizu N, Shima A: **The medaka rs-3 locus required for scale development encodes ectodysplasin-A receptor.** *Curr Biol* 2001, **11**:1202-1206.
26. Wright S: **Evolution in Mendelian Populations.** *Genetics* 1931, **16**:97-159.
27. Sabeti PC, Schaffner SF, Fry B, Lohmueller J, Varilly P, Shamovsky O, Palma A, Mikkelsen TS, Altshuler D, Lander ES: **Positive natural selection in the human lineage.** *Science* 2006, **312**:1614-1620.
28. Han Y, Gu S, Oota H, Osier MV, Pakstis AJ, Speed WC, Kidd JR, Kidd KK: **Evidence of positive selection on a class I ADH locus.** *Am J Hum Genet* 2007, **80**:441-456.
29. Oota H, Pakstis AJ, Bonne-Tamir B, Goldman D, Grigorenko E, Kajuna SL, Karoma NJ, Kungulilo S, Lu RB, Odunsi K, *et al.*: **The evolution and population genetics of the ALDH2 locus: random genetic drift, selection, and low levels of recombination.** *Ann Hum Genet* 2004, **68**:93-109.
30. Myles S, Tang K, Somel M, Green RE, Kelso J, Stoneking M: **Identification and analysis of genomic regions with large between-population differentiation in humans.** *Ann Hum Genet* 2008, **72**:99-110.

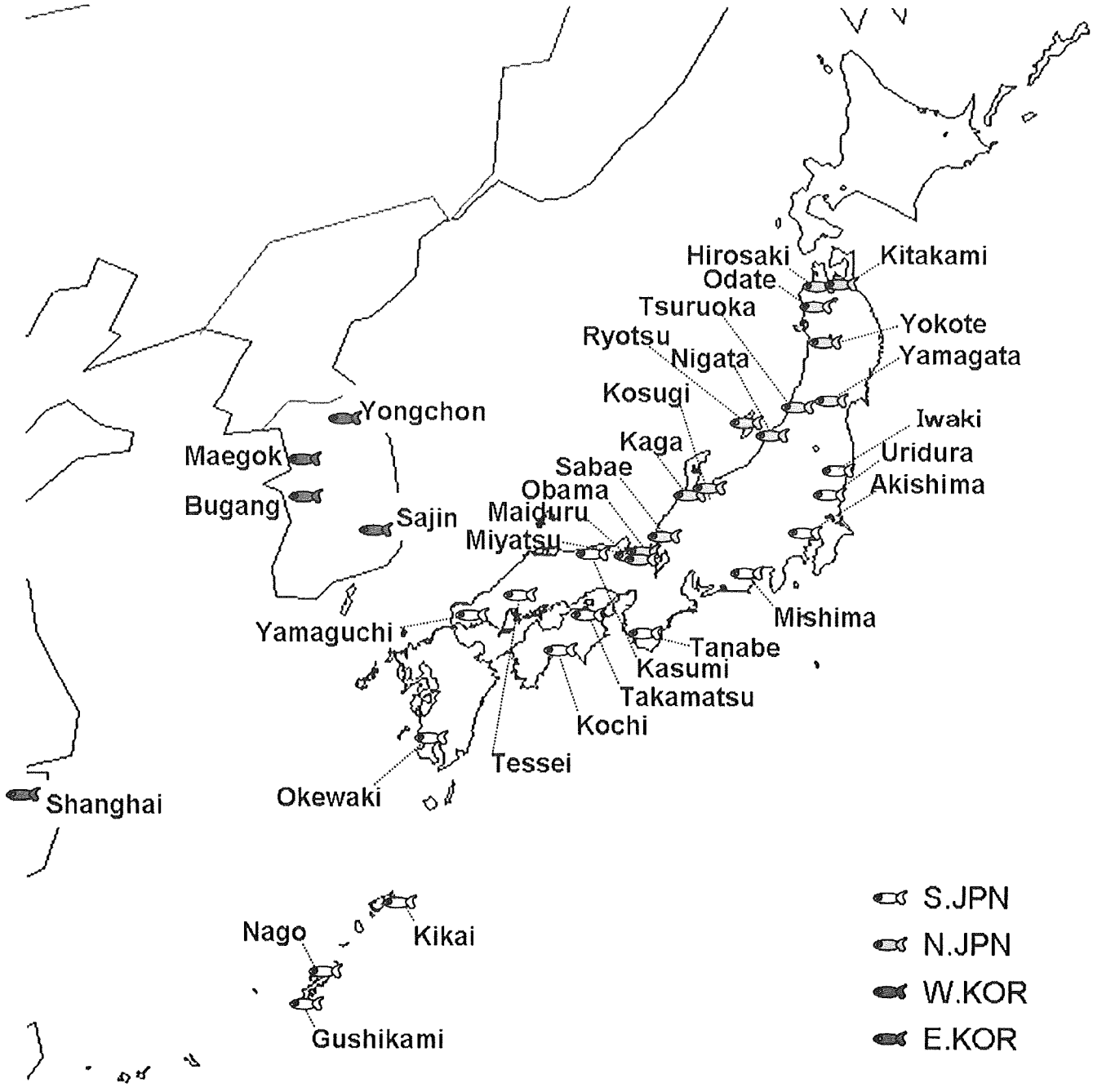
Hirosaki
Kitakami
Odate
Tsuruoka
Yokote
Ryotsu
Nigata
Yamagata
Kosugi
Yongchon
Iwaki
Kaga
Maegok
Uridura
Sabae
Akishima
Obama
Bugang
Maiduru
Sajin
Miyatsu
Mishima
Yamaguchi
Tanabe
Kasumi
Takamatsu
Kochi
Tessei
Shanghai
Okewaki
Nago
Kikai
Gushikami
S.JPN
N.JPN
W.KOR
E.KOR

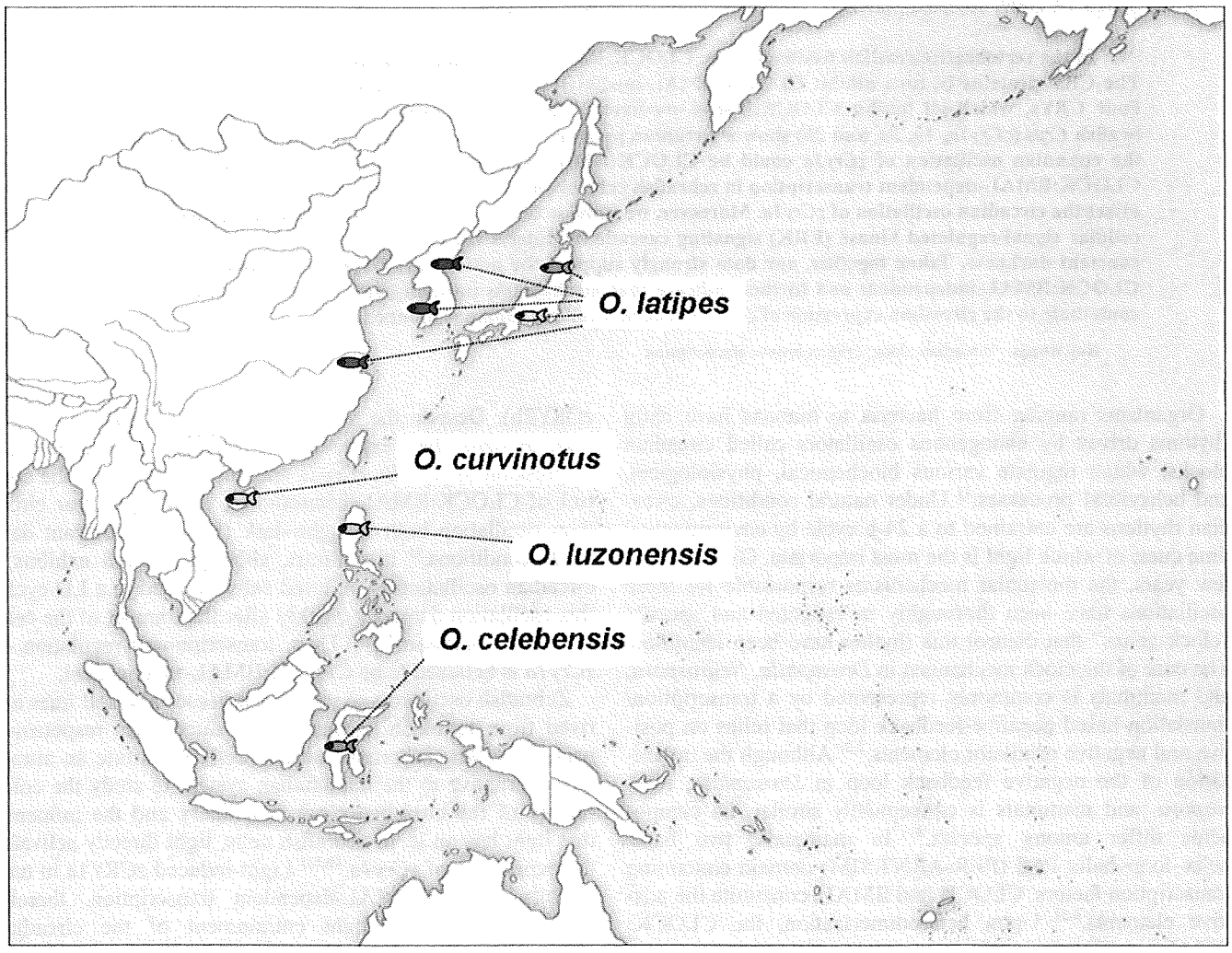
O. latipes
O. curvinotus
O. luzonensis
O. celebensis

CLOCK:BMAL-Independent Circadian Oscillation of Zebrafish *Cryptochrome1a* Gene

Norio MIYAMURA,[a,#] Jun HIRAYAMA,*[,b,#] Kenji SAWANOBORI,[a,c] Teruya TAMARU,[d] Yoichi ASAOKA,[a] Reiko HONDA,[b] Takuro YAMAMOTO,[e] Hatsume UNO,[e] Ken TAKAMATSU,[d] and Hiroshi NISHINA[a]

[a] *Department of Developmental and Regenerative Biology, Tokyo Medical and Dental University;* [b] *Medical Top Track Program, Medical Research Institute, Tokyo Medical and Dental University; 1–5–45 Yushima, Bunkyo-ku, Tokyo 113–8510, Japan:* [c] *Department of Physiological Chemistry, Graduate School of Pharmaceutical Sciences, University of Tokyo; 7–3–1 Hongo, Bunkyo-ku, Tokyo 113–0033, Japan:* [d] *Department of Physiology, Toho University School of Medicine; 5–21–16 Ohmori-nishi, Ohta-ku, Tokyo 143–8540, Japan and* [e] *Life Science Laboratory, Advanced Materials Laboratories, Sony Corporation; 1–5–45 Yushima, Bunkyo-ku, Tokyo 113–8510, Japan.*

Received March 19, 2009; accepted March 31, 2009; published online April 1, 2009

In the vertebrate circadian feedback loop, CLOCK:BMAL heterodimers induce the expression of *Cry* genes. The CRY proteins in turn inhibit CLOCK:BMAL-mediated transcription closing the negative feedback loop. Four CRYs, which all inhibit CLOCK:BMAL-mediated transcription, exist in zebrafish. Although these zebrafish *Crys* (*zCry1a*, *1b*, *2a*, and *2b*) show a circadian pattern of expression, previous studies have indicated that the circadian oscillation of *zCry1a* could be CLOCK:BMAL-independent. Here we show that abrogation of CLOCK:BMAL-dependent transcription in zebrafish cells by the dominant negative zCLOCK3-DeltaC does not affect the circadian oscillation of *zCry1a*. Moreover, we provide several lines of evidence indicating that the extracellular signal-regulated kinase (ERK) signaling cascade modulates the circadian expression of *zCry1a* gene in constant darkness. Taken together, our data strongly support the notion that circadian oscillation of *zCry1a* is CLOCK:BMAL-independent and further indicate that mechanisms involving non-canonical clock genes could contribute to the circadian expression of *zCry1a* gene in a cell autonomous manner.

Key words circadian clock; *cryptochrome*; transcription

Organisms ranging from bacteria to humans have daily rhythms driven by endogenous oscillators called circadian clocks, which regulate various biochemical, physiological, and behavioral processes.[1] Under natural conditions, circadian rhythms are entrained to a 24-h cycle by environmental time cues, of which light is the most important. Over the past few years, the molecular mechanisms responsible for these oscillations have been thoroughly investigated and specific "clock genes" that control this rhythm have been identified. The core of the clock mechanism in *Drosophila*, *Neurospora*, and mammals is commonly represented by a transcription/translation-based negative-feedback loop that relies on positive and negative oscillator elements.[2,3] Although the organization of the negative feedback loop in *Drosophila*, *Neurospora*, and mammals is conceptually similar, its components differ among species.[3] In mammals, two basic helix–loop–helix PAS (PER-ARNT-SIM) domain-containing transcription factors, CLOCK and BMAL, constitute the positive elements.[4,5] Upon heterodimerization, the CLOCK:BMAL complex drives the transcription of the negative components of the clock machinery, two *Cryptochrome* genes (*Cry1* and *Cry2*). CRYs negatively regulate their own expression, therefore setting up the rhythmic oscillations of gene expression that drive the circadian clock.[6]

Zebrafish possess an intrinsic autonomous oscillator that consists of components similar to those of mammals.[7] zCLOCK and zBMAL act as positive elements and zCRYs act as negative regulators. As the result of whole-genome duplication during the evolution of the teleost lineage, the circadian oscillator of zebrafish contains duplications for most of the clock genes. Interestingly, zebrafish have four repressor types of CRYs (zCRY1a, zCRY1b, zCRY2a, and zCRY2b). Despite the structural and functional similarities seen *in vitro*, their expression profiles are quite different.[7] Expression of *zCry1b*, *zCry2a* and *zCry2b* are under the control of CLOCK:BMAL heterodimer, showing a clear circadian oscillation both in light–dark (LD) and constant dark (DD) conditions.[8] In contrast, although *zCry1a* exhibits a circadian oscillation in cultured cells exposed to a LD cycle, this oscillation dampens quickly after the transfer of the cells to a DD condition.[9—11] Thus, transcriptional regulation of *zCry1a* is believed to be CLOCK:BMAL-independent.

Zebrafish oscillators in peripheral tissues and cell lines derived from zebrafish tissues display direct-light responsiveness.[12] In fact, zebrafish cultured cells constitute an attractive alternative to the mammalian system to study the complexity of the circadian clock machinery and the influence that light has on it. In zebrafish cells, light directly activates the expression of *zCry1a*.[10,11] Light-induced zCRY1a in turn inhibits CLOCK:BMAL-dependent transcription, thereby participating in the light entrainment of the circadian clock.[10,11] Moreover, a critical role for extracellular signal-regulated kinase (ERK) signaling pathway in the circadian transcriptional regulation has been established in a variety of species.[9,13] Indeed, we have previously reported that light-induced *zCry1a* expression is achieved through activation of the ERK signaling cascade,[11] showing the critical role of ERK pathway in transcriptional regulation of *zCry1a* gene.

Here we report that the oscillation of *zCry1a* gene expression does not depend on CLOCK:BMAL transcriptional activation. Indeed, the abolishment of CLOCK:BMAL-transactivation capacity through the expression of a dominant negative form of zCLOCK3 (zCLOCK3-DeltaC) lacking its transactivation domain does not show any impact on the cir-

* To whom correspondence should be addressed. e-mail: hirayama.mtt@mri.tmd.ac.jp
# These authors contributed equally to this work.

cadian expression of *zCry1a* gene. Furthermore, additional results indicate that ERK signaling pathway could contribute to the circadian regulation of *zCry1a* expression in constant conditions. These findings are consistent with the idea that the circadian oscillation of *zCry1a* gene is CLOCK:BMAL-independent, and further indicate that the autonomous circadian expression of *zCry1a* gene could be achieved by mechanisms involving non-canonical clock genes.

MATERIALS AND METHODS

Cells, Transfection, and Luciferase Assay Zebrafish cultured cells were prepared as described previously.[14] Briefly, cells were cultured at 28 °C in L-15 medium (Invitrogen) containing 10% foetal bovine serum. 293T cells were grown in Dulbecco's modified Eagle's medium (Invitrogen) supplemented with 10% fetal bovine serum. Zebrafish cultured cells were plated in 24-well plates and were transfected on the following day with 20 ng of firefly luciferase reporter plasmid, 5 ng of sea pansy luciferase reporter plasmid (pRL-CMV (Promega)), and expression plasmids (indicated in each figure), by the use of Fugene HD (Roche). The upstream sequence of the Period1 gene was fused to a luciferase reporter.[15] The dual luciferase assays, using the dual-luciferase reporter assay system (Promega), were performed 24 h after transfection. Firefly and sea pansy luciferase activities were quantified by means of a luminometer, with the firefly luciferase activity normalized for transfection efficiency based on the sea pansy luciferase activity. All experiments were done three times. The plasmids used in this study have been described elsewhere.[8]

Quantitative Real-Time Reverse Transcription-Polymerase Chain Reaction (RT-PCR) Total RNA extraction was done using TRIzol (Invitrogen) according to the manufacturer's instructions. Total RNA was then reverse-transcribed into cDNA by using Superscript II Reverse Transcriptase (Invitrogen) with oligo random hexamers. Each quantitative real-time RT-PCR was performed using the Chromo4 real time detection system (BIO-RAD). The PCR primers used in this study were as follows: *zPer1* FW; 5′-CAACGGAGAGGGAGAACGATGGAC-3′, *zPer1* RW 5′-GACTGAATGACACTGAGCTGCTCG-3′, *zActin* FW; 5′-GCAGATGTGGATCAGCAAGCAGG-3′, *zActin* RW 5′-C-TGAGTCAATGCGCCATACAGAG-3′, *zPer2* FW; 5′-GAA-AGGACAGGTCACGTCTGAAGC-3′, *zPer2* RW 5′-TGA-TGGAGTGCTGTCTGACGACTC-3′, *zCry1a* FW; 5′-GAC-GCACAGCAGATAACAGGAC-3′, and *zCry1a* RW 5′-GA-CCTGATGTTTAGGAGCTGCAC-3′. For a 20 μl PCR, cDNA template was mixed with the primers to final concentrations of 200 nM and 10 μl of iQ SYBR Green Supermix (BIO-RAD), respectively. The reaction was first incubated at 95 °C for 3 min, followed by 40 cycles at 95 °C for 15 s, 60 °C for 15 s, and 72 °C for 20 s.

Antibodies Myc (9E10), green fluorescent protein (GFP), and actin antibodies were purchased from Santa Cruz, ERK antibody from Cell Signaling, phospho-ERK antibody from New England Biolabs, and Flag antibody from Sigma.

Co-immunoprecipitation Co-immunoprecipitation was done as previously described,[16] with some modifications. 293T cells were seeded in 10-cm dishes and were transfected the following day with the expression plasmids described in Fig. 1B. Twenty-four hours after transfection cells were washed twice with phosphate-buffered saline (PBS), homogenized in binding buffer (150 mM NaCl, 1 mM ethylenediaminetetraacetic acid (EDTA), 0.5% Nonidet P-40, 1 mM ethylene glycol bis(2-aminoethyl ether)-*N*,*N*,*N*′,*N*′-tetraacetic acid (EGTA), 5% glycerol, and 20 mM Tris–HCl pH 7.4) containing protease inhibitor mixture tablets, and then clarified by centrifugation for 10 min at 15000×***g***. Total protein from the supernatant was incubated with 15 μl of protein G-agarose beads (Amersham Biosciences) for 1 h at 4 °C, after which the material was centrifuged. The supernatant was incubated for 12 h at 4 °C with Flag antibody and 20 μl of protein G-agarose beads. The beads were then washed three times with binding buffer and boiled in sodium dodecyl sulfate (SDS) sample buffer. The supernatant was separated by SDS-PAGE and analyzed by Western blotting, as described below.

Western Blotting The immunoprecipitated material and total cell lysate extracted as described above were separated by SDS-PAGE and transferred electrophoretically onto a polyvinylidene difluoride membrane. The membrane was blocked with 2% or 5% nonfat milk and incubated with each of the antibodies described in each figure for 10 h at 4 °C. The blots were incubated with the appropriate secondary antibody, peroxidase-conjugated anti-mouse or anti-rabbit immunoglobulin (Ig)G antibody (Santa Cruz), and developed with the ECL Western blotting detection system (Amersham Biosciences).

Retroviral Infection The RetroMax expression system (IMGENEX) was used to produce retrovirus according to the manufacturer's instructions. Flag-Myc-tagged *zClock3* gene (nucleotides 1-1758) was cloned into pCLNCX retroviral vector, in which the cloned gene is under the control of the CMV promoter. We used pMD.G/vsv-g as enveloping vector. Infection efficiency (95—100%) was confirmed thanks to a pCLNCX retroviral vector expressing GFP and neomycin selection in zebrafish cultured cell as described previously.[11]

RESULTS AND DISCUSSION

The zCLOCK3-DeltaC Is a Dominant Negative Effector for CLOCK:BMAL-Dependent Transcription CLOCK and BMAL1 heterodimerize to form an active transcription complex to mediate circadian transcription.[1] The N-terminal part of the CLOCK protein has two PAS domains required for heterodimerization with BMAL and the C-terminal part has the transactivation domain.[4] In order to test whether zCry1a is direct transcriptional target of CLOCK:BMAL, we decided to generate a dominant-negative form of CLOCK. For this, we constructed a truncated form of zebrafish CLOCK3 (zCLOCK3-DeltaC) lacking its C-terminal transactivation domain (amino acids 586—773) (Fig. 1A). As expected, the zCLOCK3-DeltaC retained the ability to bind BMAL (Fig. 1B), but zCLOCK3-DeltaC:BMAL complex showed a markedly reduced transactivation capacity (Fig. 1C). We speculated that over-expression of zCLOCK3-DeltaC in cultured cells would block the formation of active CLOCK:BMAL complexes by squelching endogenous BMAL proteins, therefore leading to the abrogation of CLOCK:BMAL-dependent transcription. To test this hypothesis, we infected zebrafish cultured cells with a retroviral

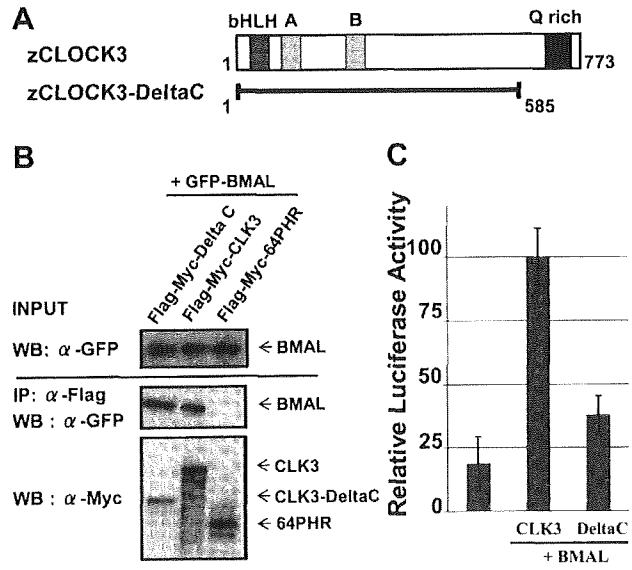

Fig. 1. Characterization of the C-Terminally-Truncated zCLOCK3, zCLOCK3-DeltaC

(A) Schematic representation of zCLOCK3 protein showing the positions of basic helix–loop–helix (bHLH) motif, Per-Arnt-Sim (PAS) domains, the glutamine-rich (Q-rich) region and the construct of the deletion mutant. Numbers indicate the amino acid residues in the protein of origin. (B) Flag-Myc-CLOCK3, Flag-Myc-CLOCK3-DeltaC, or Flag-Myc-64photolyase (64PHR) was co-expressed with GFP-BMAL1 in cultured cells. The cell lysates were immunoprecipitated (IP) with the Flag antibody. Immunoprecipitated material was analyzed by Western blotting (WB) with anti-GFP (GFP-BMAL1) or anti-Myc (Flag-Myc-CLOCK3, Flag-Myc-CLOCK3-DeltaC, or Flag-Myc-64PHR). Analyses of total cell lysate with anti-GFP antibody confirmed the equal expression of GFP-BMAL1 (top panel). 64PHR protein was used as negative control of the experiment. (C) The transactivation ability of CLOCK3:BMAL and CLOCK3-DeltaC:BMAL complexes was examined in a luciferase reporter gene assay. The reporter plasmid was co-transfected with the expression vectors shown. Values are means±S.E.M. of three independent experiments. In each experiment, the luciferase activity of the CLOCK3:BMAL-containing sample was adjusted to 100%.

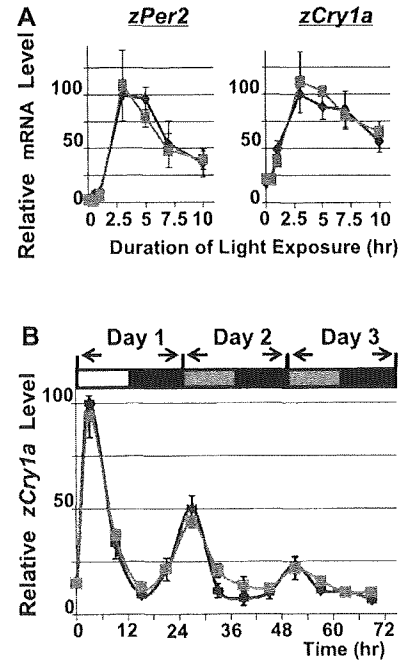

Fig. 3. Effects of zCLOCK3-DeltaC on Transcription of *zCry1a* Gene

(A) Light induction of *zPer2* and *zCry1a* expression in *zClock3-DeltaC*-(square) and *Gfp*-(circle) infected zebrafish cultured cells was examined by RT-qPCR analysis. Zebrafish cultured cells maintained in constant darkness were exposed to light, and RNA was harvested at each time point indicated after light onset. The value from the cells at time point 3 was set as 100% for each gene, and zebrafish actin gene was used for normalization. (B) Oscillation of *zCry1a* gene in *zClock3-DeltaC*-(square) and *Gfp*-(circle) infected zebrafish cultured cells was examined. Cells maintained in constant darkness were exposed to LD condition for 1 d and then transferred to DD condition for another 2 d. RNA was harvested at each time point indicated. *zCry1a* gene expression was examined by RT-qPCR analysis. The value from the cells at time point 3 h was set as 100%. Each value is the mean±S.E.M. of three independent experiments.

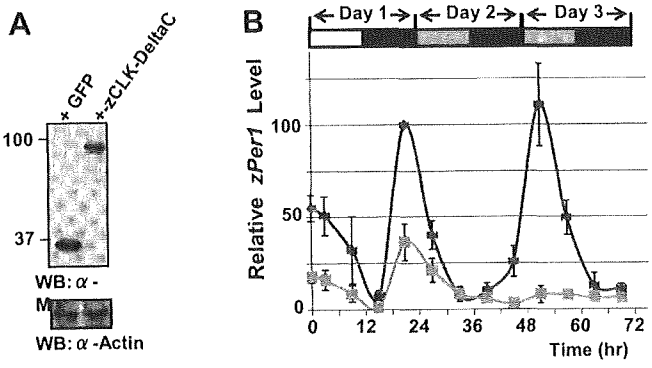

Fig. 2. Effect of zCLOCK3-DeltaC on Transcription of *zPer1* Gene

(A) Expression of retrovirally-infected Myc-GFP or Myc-zCLOCK3-DeltaC in zebrafish cultured cells was confirmed by Western blotting (WB) with anti-Myc (upper panel). The same cell lysates were immunoblotted with an antibody against actin as a loading control (lower panel). (B) Oscillation of *zPer1* gene in *zClock3-DeltaC*-(square) and *Gfp*-(circle) infected zebrafish cultured cells was examined. Cells maintained in constant darkness were exposed to LD condition for 1 d and then transferred to DD condition for another 2 d. RNA was harvested at each time point indicated. *zPer1* gene expression was examined by RT-qPCR analysis. The relative RNA value from cells at 24 h was set as 100%. Each value is the mean±S.E.M. of three independent experiments. The bar above the blots indicates light (white), subjective day (grey), and subjective night (black) periods. We used GFP-infected cell as a control of retroviral infection. The infection of GFP did not show any effect on both the light induction and the circadian oscillation of gene expression in zebrafish cultured cells as previously reported[11] (data not shown).

vector (pCLNCX-*zClock3-DeltaC*) encoding the *zClock3-DeltaC* gene (Fig. 2A) and analyzed the expression of a well-known CLOCK:BMAL target gene, *zPer1*,[14,17] in *zClock3-DeltaC* infected cells. In control cells, *zPer1* expression showed a clear circadian oscillation both in LD and DD conditions as expected (Fig. 2B). This circadian oscillation of *zPer1* was markedly diminished in cultured cells over-expressing zCLOCK3-DeltaC, showing that zCLOCK3-DeltaC works as a dominant negative effector for CLOCK:BMAL-dependent transcription in zebrafish cultured cells.

zCLOCK3-DeltaC Does Not Affect the Light-Dependent Induction or the Circadian Oscillation of *zCry1a* Expression We next tested the effect of zCLOCK3-DeltaC over-expression on the light induction of *zCry1a* and *zPer2* genes, which has been reported to be mediated by activation of the ERK signaling pathway.[9,11] As previously reported,[9–11] light strongly induced the expression of the two genes and the light inducibility of both *zCry1a* and *zPer2* were not affected by zCLOCK3-DeltaC over-expression (Fig. 3A), indicating that CLOCK:BMAL complex is not involved in the light-dependent expression of *zCry1a* and *zPer2* genes. Interestingly, this finding is not entirely in agreement with a previous report showing that, in a mammalian system, both the ERK signaling cascade and CLOCK:BMAL complex positively contribute to the light-induction of clock-controlled genes.[18] We can therefore speculate that the effect of ERK signaling on the transcriptional regulation of clock genes may be dominant over the one exerted by the oscillatory machinery for controlling the light-dependent expression of circadian clock genes in zebrafish.

Interestingly, in zebrafish cells, even though *zCry1a* ex-

pression exhibits a clear circadian pattern in a LD cycle, the amplitude of its oscillation quickly dampens once the cells are transferred to DD conditions[10,11] (Fig. 3B). This oscillatory profile is quite different from that of *zPer1* and the other *zCrys*, whose expression is directly regulated by the CLOCK:BMAL complex and shows a robust circadian oscillation both in LD and DD conditions.[8,14] Based on these observations, we hypothesized that the circadian oscillation of *zCry1a* in DD conditions could be CLOCK:BMAL-independent. To test the possibility, we analyzed the temporal expression pattern of *zCry1a* in the cells over-expressing zCLOCK3-DeltaC. Interestingly, the *zCry1a* expression showed a similar circadian pattern in cells over-expressing zCLOCK3-DeltaC and in control cells, consistent with the idea that the circadian expression of *zCry1a* is CLOCK:BMAL-independent.

Notably, zCRY1a directly interacts with CLOCK:BMAL complex and represses transcription mediated by the complex.[10,19] Thus, our finding of a CLOCK:BMAL-independent *zCry1a* regulation indicates that expression of *zCry1a* is specifically regulated by a non-circadian cellular mechanism, which could modulate core circadian clock transcription by the control of *zCry1a* expression. In support of this notion, light activates ERK signaling pathway to induce *zCry1a* expression.[9,11] The induced zCRY1a then inhibits CLOCK:BMAL-dependent transcription, participating in the light entrainment of circadian clock.[10] Indeed, ERK signaling cascade regulates a variety of physiological responses to extracellular signals, such as DNA damage and nutrient conditions.[20,21] Conceivably, we envisage a scenario where zCRY1a acts as a signaling mediator integrating a variety of environmental cues to the core circadian machinery, the CLOCK:BMAL complex, therefore modulating the circadian machinery under different physiological conditions.

ERK Signaling Cascade Modulates *zCry1a* Circadian Oscillation We next sought to investigate the signaling pathways participating in the circadian oscillation of *zCry1a* in DD conditions. Interestingly, it has been reported that circadian activation of ERK is autonomously regulated in the suprachiasmatic nuclei (SCN), the central circadian pacemaker in mammals.[22,23] This finding, together with our previous observation that ERK mediates light-induction of *zCry1a* expression,[11] suggests that ERK signaling cascade could also contribute to the transcriptional regulation of *zCry1a* gene in DD conditions. In order to address this, we first tested the temporal pattern of ERK phosphorylation in zebrafish cultured cells. The cells were exposed to LD cycle for 1 d and then transferred to DD conditions. Cell extracts were then prepared at several time points after the transfer of the cells to a DD condition and the ERK phosphorylation levels were examined by Western blotting. Interestingly, ERK phosphorylation displayed a remarkable oscillation, evidence of a cell-autonomous regulation of the ERK activation state in zebrafish (Fig. 4A). Notably, ERK phosphorylation levels increased when *zCry1a* gene expression was down-regulated (Figs. 3B, 4A), indicating that the ERK signaling cascade may negatively regulate *zCry1a* expression in DD conditions.

We next examined if the circadian phosphorylation of ERK would contribute to the transcriptional regulation of *zCry1a* in DD condition by the means of a MEK/ERK specific inhibitor, U0126. As expected, cells treated with U0126

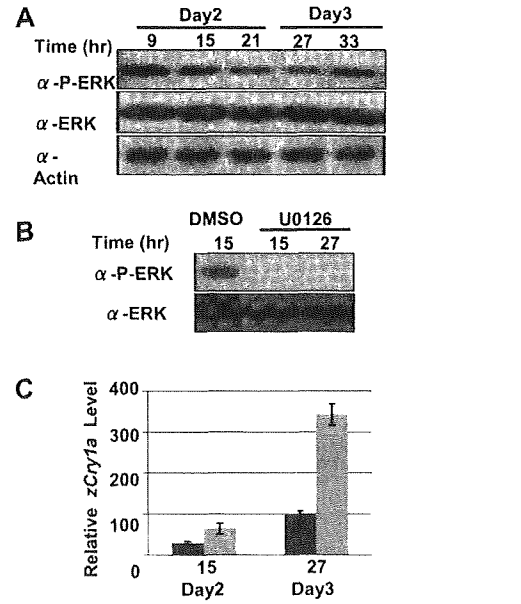

Fig. 4. The Role of ERK Signaling Cascade in Circadian Oscillation of *zCry1a* in DD Condition

(A) Temporal pattern of ERK phosphorylation state in zebrafish cultured cells was examined. The zebrafish cultured cells were cultured in LD condition for 1 d and then transferred to DD condition. At indicated time points after transferring the cells to DD condition, cells were harvested for Western blotting (WB) with anti-phospho-ERK (upper panel), anti-ERK (middle panel), or anti-actin (lower panel). Similar results were found in replicate experiments. (B) ERK phosphorylation state was examined in zebrafish cultured cell treated with U0126 (30 μM) as described in (A). Cells were treated with U0126 (30 μM) 13 h after placing the cells in DD conditions. At indicated time points after the onset of DD conditions, cells were harvested for Western blotting. Similar results were found in replicate experiments. (C) Effect of U0126 inhibitor on *zCry1a* expression. Expression level of *zCry1a* gene was examined in zebrafish cultured cells treated with the U0126 (gray bar) or with the vehicle (DMSO, black bar). Cells were treated with U0126 (30 μM) 13 h and placed in DD conditions. At indicated time points after transferring cells to DD condition, cells were harvested for RT-qPCR analysis. The value from the cells at time point 27 treated with vehicle was set as 100%. Each value is the mean±S.E.M. of three independent experiments.

did not display any levels of phosphorylated ERK (Fig. 4B). Importantly, the expression level of *zCry1a* was increased in cells treated with U0126 (Fig. 4C), showing that ERK signaling pathway modulates in a negative manner the transcription of *zCry1a* in DD condition. It should be emphasized that, although U0126 inhibitor enhanced *zCry1a* expression, the expression level of *zCry1a* at time point 15 was much lower than that at time point 27, suggesting that ERK signaling pathway would not be the only regulator for *zCry1a* transcription. In fact, the promoter region of *zCry1a* gene contains multiple regulatory elements.[11] It is therefore conceivable that other cellular signaling cascades and transcription factors would contribute to *zCry1a* transcription. Identification of these signaling pathways and transcription factors will provide a clearer understanding of the molecular mechanism of *zCry1a* circadian expression.

Our results suggest that ERK signaling pathway negatively regulates *zCry1a* transcription in DD conditions, as the specific MEK/ERK inhibitor U0126 enhanced the expression of *zCry1a* (Fig. 4C). In contrast, the light-dependent activation of ERK signaling cascade induces *zCry1a* expression.[11] This apparent contradiction could be reconciled if we think that the light-dependent and cell-autonomous ERK activating pathways may direct ERK to phosphorylate different targets, which could in turn regulate *zCry1a* transcription in opposite directions. In support of this notion, ERK signaling cascade